Calorimetric study of the effect of bent-shaped dopant molecules on the critical behavior at the nematic-smectic-A_d phase transition

Y. Sasaki and K. Ema*
Department of Physics, Tokyo Institute of Technology, O-okayama, Meguro, 152-8551 Japan

K. V. Le and H. Takezoe
Department of Organic and Polymeric Materials, Tokyo Institute of Technology, O-okayama, Meguro, Tokyo 152-8552, Japan

S. Dhara
School of Physics, University of Hyderabad, Hyderabad-500 046, India

B. K. Sadashiva
Raman Research Institute, C. V. Raman Avenue, Bangalore 560 080, India

(Received 23 December 2010; revised manuscript received 29 March 2011; published 8 June 2011)

We report results of calorimetric studies for the binary mixture of rodlike host *n*-alkyloxy-cyanobiphenyl (*n*OCB, $n = 8,9$) and bent-shaped guest 1,3-phenylene-bis[4-(3-methylbenzoyloxy)]-4′-*n*-dodecylbiphenyl-4′-carboxylate (BC12). The effect of bent-shaped dopant molecules on the critical behavior associated with the nematic-smectic-A_d phase transition has been studied in detail. The transition temperature for the nematic-smectic-A_d phase sharply decreases as the increase of the mole fraction of the dopant concentration (denoted X for the BC12/9OCB mixture and Y for the BC12/8OCB mixture). The dependence of the critical exponent α on X and Y is well explained in terms of the McMillan ratio. A nearly tricritical exponent has been obtained for the $X = 0.01$ mixture. $X = 0.02 - 0.03$ mixtures, pure 8OCB, and $Y = 0.01 - 0.03$ mixtures exhibit nonuniversal behaviors with effective exponents lying between the 3D-XY and tricritical exponents. The heat capacity anomaly for $Y = 0.05$ has been well described with the 3D-XY exponent. The critical amplitude ratio A^-/A^+ is close to 1 and insensitive to the dopant concentration. No Fisher renormalization of the critical exponent has been observed even for nearly tricritical compositions, which indicates the smallness of the concentration plays a decisive role rather than the steepness of the N-SmA_d phase boundary.

DOI: 10.1103/PhysRevE.83.061701 PACS number(s): 64.70.M−, 64.60.F−, 65.40.Ba

I. INTRODUCTION

Recent research into liquid crystalline binary mixtures composed of bent-shaped and rodlike molecules has shown various interesting phenomena such as novel phase transitions [1,2] and nanophase segregations [3–5]. On the other hand, the exact treatment of phase transitions in such mixture systems is complicated because measurements are usually performed along with a constant concentration x, while fixing the chemical potential difference in the mixture significantly acts as a thermodynamic constraint. As Fisher discussed [6,7], the heat capacity exponent α is modified as $\alpha_x = -\alpha/(1-\alpha)$ in the vicinity of the transition temperature T_c, which is known as the Fisher renormalization. So far, this phenomenon has been observed in rodlike liquid crystalline mixtures at the nematic (N)-smectic-A (SmA) phase transition [8–10] and smectic-A_1-smectic-A_2 phase transition [11,12]. In addition, recently, the present authors have carried out high-resolution calorimetric studies on a novel orientational phase transition of bent-shaped molecules in a smectic liquid crystal matrix [13]. It has been found that the heat capacity anomaly can be described with Fisher-renormalized form in the vicinity of T_c and that the magnitude of α plays a significant role as found in several systems [6,8,14].

A detailed estimation [15] regarding the crossover temperature between the Fisher renormalization and the underlying critical behavior can be written as

$$\tau = \left[Ax(1-x)\left(\frac{1}{T_c}\frac{dT_c}{dx}\right)^2 \right]^{1/\alpha}, \qquad (1)$$

where A is the unrenormalized critical amplitude of specific heat in units of R. This indicates that the extent of the renormalization strongly depends on the magnitude of several parameters, not only $T_c^{-1} \cdot dT_c/dx$, but also α, etc. In particular, it can also be noticed from Eq. (1) that the concentration x itself plays an important role. The crossover temperature becomes small with decreasing concentration, so that it can happen that no renormalization can be observed experimentally, even for the tricritical exponent. Somehow, almost all earlier reports mainly discussed the observation of Fisher renormalization with respect to the steepness of the phase boundary. Thus the importance of the concentration still remains ambiguous and should be examined experimentally to obtain a quantitative conclusion.

In this paper we report the results of intensive calorimetric investigations on the N-SmA_d phase transition with bent-shaped dopant molecules. Molecular structures of the host and dopant materials are shown in Fig. 1. Rodlike liquid crystalline molecules, *n*-alkyloxy-cyanobiphenyl (8OCB) and (9OCB), have been used as host compounds. Bent-shaped

*kema@phys.titech.ac.jp

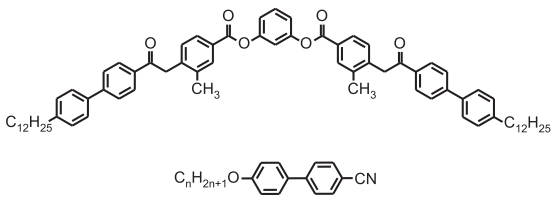

FIG. 1. Structures of (upper) bent-core dopant molecule 1,3-phenylene-bis[4-(3-methylbenzoyloxy)]-4′-*n*-dodecylbiphenyl-4′-carboxylate (BC12) and (lower) rodlike molecule n-alkyloxy-cyanobiphenyl (*n*OCB, $n = 8,9$).

molecules (1,3-phenylene-bis[4-(3-methylbenzoyloxy)]-4′-*n*-dodecylbiphenyl-4′-carboxylate; BC12) has been used as a dopant in the rodlike molecules. The overall phase diagram of the BC12/8OCB system has been reported in Ref. [2]. We particularly focus on the region where the concentration of the bent-shaped molecules is small. In both systems, it has been found that doping of the bent-shaped molecules gives rise to a sharp decrease of the N-SmA_d transition temperature T_{NA} and a gradual increase of the isotropic (I)-N phase transition temperature T_{IN}. For clarity, we use hereafter the notation X for the BC12/9OCB and Y for the BC12/8OCB mixtures to denote the mole fraction of BC12. The detailed analysis for the N-SmA_d critical behavior revealed that the dependence of the critical exponent on X and Y has been well described in terms of the McMillan ratio $r = T_{NA}/T_{IN}$. The crossover of α from tricritical ($\alpha_{\rm TCP} = 0.5$) to 3D-XY ($\alpha_{XY} = -0.0066$ [16,17]) values has been observed by mixing a small amount of bent-shaped molecules. On the other hand, no sign of the Fisher renormalization of the critical exponent has been found, even for the nearly tricritical cases. This indicates that, despite the steep phase boundary, the smallness of the concentration plays a decisive role and hinders the observation of the renormalized critical exponent.

II. METHODS AND RESULTS

The measurements have been done using two techniques, an ac calorimetry and a heat-flux differential scanning calorimetry (DSC). The details of the ac calorimetry used in the present study are found elsewhere [18]. Basically, the precise specific heat capacity data have been obtained by measuring the magnitude of an oscillatory temperature response $\Delta T_{\rm ac} \exp i(2\pi f t + \pi/2 + \phi)$ to an input heater power $P \exp(i2\pi f t)$. Here f is the frequency of the ac heating, which has been set to 0.03125 Hz in the present study. The phase shift ϕ between the input heater power and the temperature oscillation of the sample has also been measured, which provides qualitative information for the nature of the transition [19]. Particularly, in the case of a first-order transition, it is known that ϕ exhibits an anomalous increase near the transition, as will be discussed later. The temperature scan rate in the ac calorimetry was about ± 0.03 K/h near the transition region. Another method used here, DSC, has been employed for the determination of the transition enthalpy. Semiconducting thermoelectric modules have been used for the measurement of the temperature difference between a sample cell and a reference cell. A temperature scan rate of

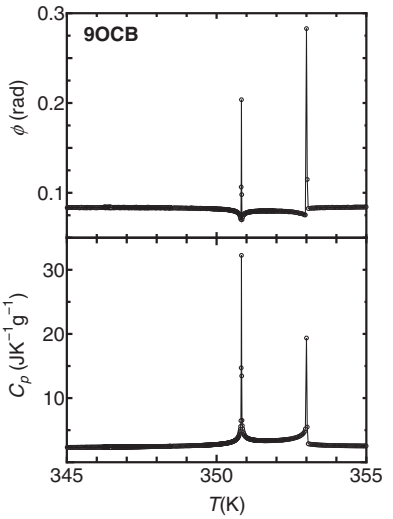

FIG. 2. Temperature dependence of the phase shift and heat capacity for pure 9OCB near the I-N and N-SmA_d phase transitions. The temperature scan rate used is 0.3 K/h for the overall range.

± 0.05 K/min has been used. Samples of about 7 mg were placed in hermetically sealed gold cells.

The specific heat C_p of the liquid crystal sample is obtained with the use of the following expression:

$$C_p = (C_p^{\rm obs} - C_p^{\rm empty})/m. \qquad (2)$$

Here $C_p^{\rm obs}$ is the observed heat capacity of the filled cell, $C_p^{\rm empty}$ is the heat capacity of the empty cell, and m is the mass of the liquid crystal sample.

The temperature variation of C_p and ϕ obtained for pure 9OCB is presented in Fig. 2. The C_p anomalies associated with the N-SmA and I-N phase transitions are evident at 350.84 and 353.03 K, respectively. The abrupt anomalous increase of the phase shift ϕ, which is characteristic of the first-order transition [20], has been observed. Such behavior is also in agreement with other N-SmA phase transitions with narrow nematic ranges [21]. The two-phase coexistence regions estimated from the ϕ anomalies are ~ 0.04 K for the N-SmA_d and ~ 0.09 K for the I-N phase transitions.

Figure 3 displays the temperature dependence of C_p and ϕ for the $X = 0.01$ mixture. The I-N phase transition exhibited essentially the same results, indicating the first-order transition, whereas, in contrast to pure 9OCB, ϕ shows a small dip near the N-SmA_d transition. Although this behavior is usually understood to indicate that the transition is second order, it is valuable to take a closer look at this because the anomaly in C_p is rather large and sharp. As discussed in Ref. [22], a linear relationship between ϕ and C_p is expected in the absence of two-phase coexistence. In Fig. 4 data near the N-SmA_d transition for pure 9OCB, $X = 0.01$, and $X = 0.03$ mixtures are plotted on a ϕ-C_p plane. In the case of pure 9OCB, data points in the immediate vicinity of the transition break the linear relation, indicating the first-order nature of the transition. On the other hand, all the data points fall on a straight line in the case of the $X = 0.03$ mixture, which ensures the absence of the two-phase coexistence. Similar results were found for mixtures with $X = 0.02$ and $Y = 0.00 - 0.05$. For the $X = 0.01$ mixture, shown in the middle portion of Fig. 4,

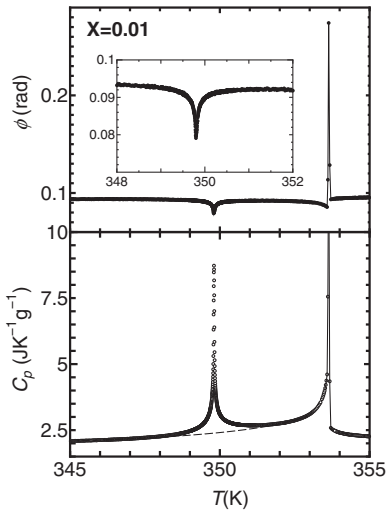

FIG. 3. Temperature dependence of the phase shift and heat capacity for the $X = 0.01$ mixture near the I-N and N-SmA_d phase transitions. The dashed curve represents the background heat capacity associated with the N-SmA_d phase transition. The temperature scan rates used are 0.03 K/h near the N-SmA_d and 0.3 K/h near the I-N phase transitions.

a slight but noticeable deviation is seen near the transition. This shows that the transition is very weakly first order in this mixture. Two-phase coexistence as determined from the above-mentioned deviation becomes rather narrow, in a range of about 0.030 K.

Figure 5 shows the N-SmA_d heat capacity anomalies obtained for various BC12/9OCB and BC12/8OCB mixtures. The heat capacity anomalies associated with the N-SmA_d transition are evident, accompanying a decrease of the transition temperatures with the increase of the concentration. As seen from the phase diagram displayed in Fig. 6, the T_{NA} value decreases sharply with increase of the dopant concentration with phase boundaries of $dT_{NA}/dX \sim -150$ K for BC12/9OCB and $dT_{NA}/dY \sim -130$ K for BC12/8OCB, which are shown as solid lines. Contrary to the N-SmA_d transition, T_{IN} monotonically increases with respect to the dopant concentration, resulting in the expansion of the nematic temperature range.

The dashed curve shown in Fig. 3 represents the estimation of the background heat capacity associated with the I-N phase transition. The excess specific heat capacity for the N-SmA_d phase transition is obtained by subtracting the contribution from the I-N phase transition C_p(background):

$$\Delta C_p = C_p - C_p(\text{background}). \tag{3}$$

A similar procedure has been also done for data on other samples.

The transition enthalpy δH in the N-SmA_d phase transition has been estimated as

$$\delta H = \Delta H_L + \int \Delta C_p \, dT. \tag{4}$$

Here ΔH_L and $\int \Delta C_p \, dT$ indicate the latent heat and the enthalpy change due to pretransitional fluctuations, respectively. Whereas ΔC_p is measured by the ac calorimetric technique, DSC directly measures δH. When the transition is second order, ΔH_L is absent, and the transition enthalpy obtained by DSC should be the same as that by ac calorimetry. For pure 9OCB, the δH value obtained by DSC shows a larger value compared with that of ac calorimetry, indicating the presence of the latent heat. Figure 7 displays the heat capacity anomalies for $X = 0.01$ and $Y = 0.02$ obtained by DSC and ac calorimetry. For the $Y = 0.02$ case, both results agree with one another on the whole and indicate a second-order transition. On the other hand, the heat capacity anomaly by DSC for $X = 0.01$ is slightly larger than that by ac calorimetry in the vicinity of T_c. This agrees with the very weak first-order nature of the transition accompanying a small latent heat, which has been expected from the ϕ-C_p plot mentioned above. Table I summarizes phase-transition temperatures T_{NA} and T_{IN}, two-phase coexistence width δT_{NA} and δT_{IN}, transition enthalpy δH_{NA}, latent heat $\Delta H_{L,NA}$, and the McMillan ratio.

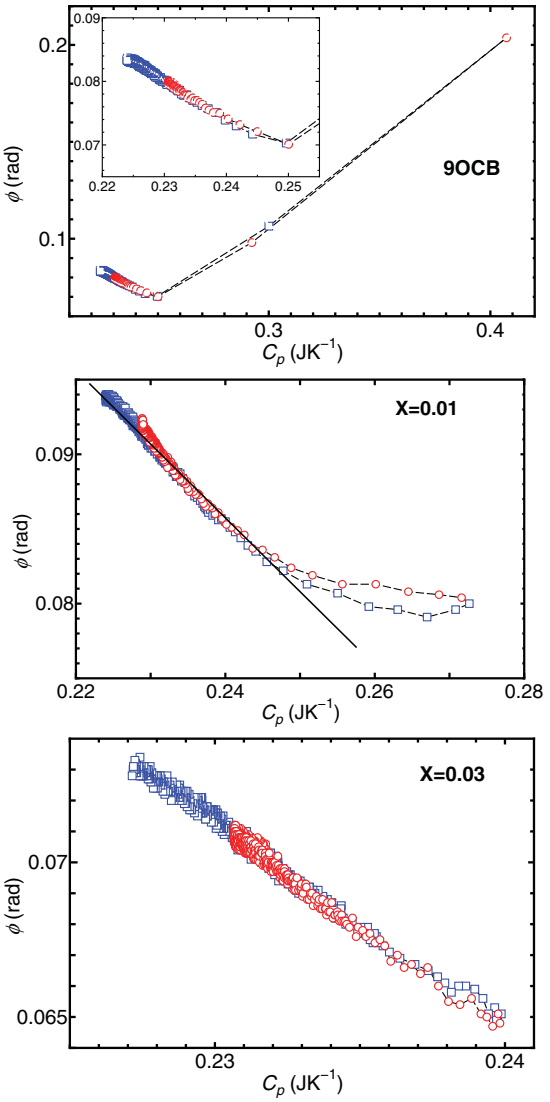

FIG. 4. (Color online) Plot of the phase lag ϕ against C_p for (upper) pure 9OCB, (middle) $X = 0.01$ mixture, and (lower) $X = 0.03$ mixture near the N-SmA_d phase transition obtained by ac calorimetry. Open circles (red) and squares (blue) represent data above and below the transition temperature.

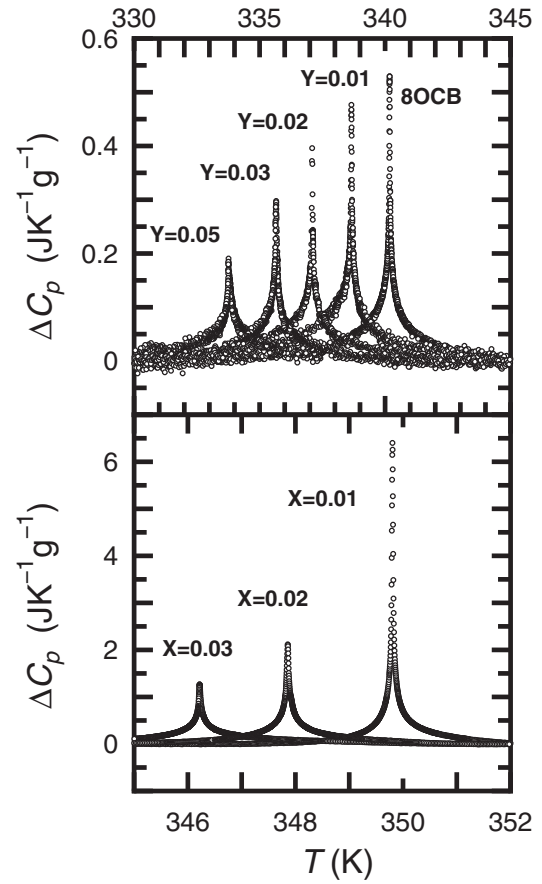

FIG. 5. Temperature variation of the excess heat capacity ΔC_p near the N-SmA_d phase transition for BC12/8OCB mixtures (upper) and for BC12/9OCB mixtures (lower) obtained by ac calorimetry.

We also add that any noticeable hysteresis indicating phase separation was not observed in all cases.

For the critical exponent analyses, the data obtained by ac calorimetry have been used. As described above, the DSC measurements also provide the high-resolution data. However, since the temperature scan rate used in our DSC measurements is faster than that of the ac calorimetric measurement, the DSC data in the very vicinity of T_c may be smeared by the finite scan

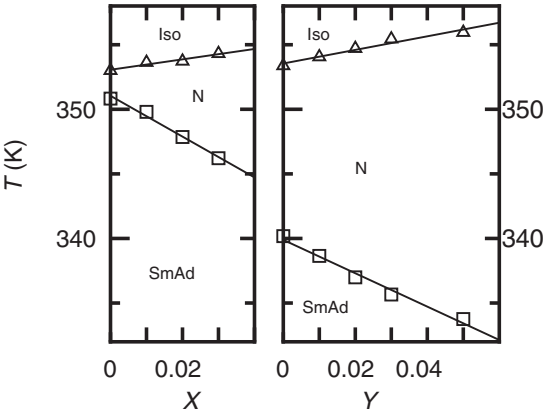

FIG. 6. Partial phase diagrams for BC12/9OCB (left) and BC12/8OCB (right). The transition temperatures have been determined by ac calorimetry.

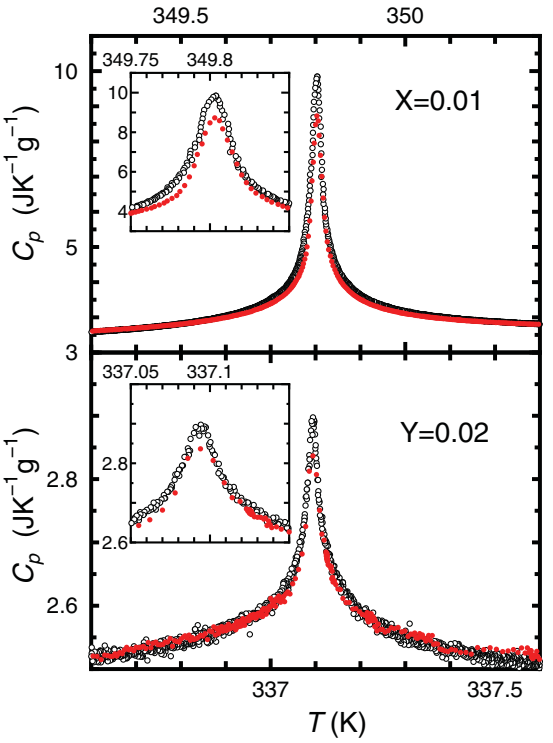

FIG. 7. (Color online) Temperature dependence of the heat capacity for mixtures $X = 0.01$ (upper) and $Y = 0.02$ (lower) near the N-SmA_d phase transitions. The closed (red) and open circles (black) represent the data obtained by ac calorimetry and DSC, respectively.

rates. The fits to the ΔC_p have been performed with the following expression, including corrections-to-scaling terms [16,23]:

$$\Delta C_p = A^{\pm}|t|^{-\alpha}\left(1 + D_1^{\pm}|t|^{\theta} + D_2^{\pm}|t|^{2\theta}\right) + B_c. \qquad (5)$$

Here $t = (T - T_c)/T_c$ is the reduced temperature, and $\pm$ indicates above and below T_c. $D_1^{\pm}$ and $D_2^{\pm}$ are the coefficients of the first- and second-order corrections-to-scaling terms, respectively. The corrections-to-scaling exponent θ is taken to be 0.5 [16,23]. The constant term B_c is the critical contribution. The data in the vicinity of the transition temperature are not used due to the instrumental limitations and the inhomogeneity of the sample. The fits to the data have been performed for $|t|_{\min} \leqq |t| \leqq |t|_{\max}$, with $|t|_{\max}$ being the maximum reduced temperature used in the fits. The $|t|_{\min}$ values have been determined according to the method described in Ref. [24]. The rounding regions thus determined are described in the caption of the tables shown below.

Table II shows the results for the $X = 0.01$ mixture. Although the transition was found to be first order for this mixture, the critical exponent analyses with Eq. (5) can be justified because the first-order nature is very weak. Indeed, two-phase coexistence width only amounts to about 30 mK, comparable to the typical rounding region found for second-order phase transitions. The fits have been carried out for several $|t|_{\max}$ values to check the dependence of the adjustable parameters on the data range. From the simple power-law fit without corrections-to-scaling terms, the critical exponent α is in the range 0.54–0.57, which is independent of the data range shrinking and slightly larger than the tricritical value $\alpha_{\mathrm{TCP}} = 0.5$. The amplitude ratio A^-/A^+ is smaller than 1.

TABLE I. Values of transition temperature T_{NA} and T_{IN}, two-phase coexistence width δT_{NA} and δT_{IN}, transition enthalpy δH_{NA}, latent heat $\Delta H_{L,NA}$, and McMillan ratio. Subscripts NA and IN represent N-SmA_d and I-N transitions, respectively. The unit is K for T_{NA}, T_{IN}, δT_{NA}, and δT_{IN}, and J/g for δH_{NA} and $\Delta H_{L,NA}$.

Sample	T_{NA}	δT_{NA}	δH_{NA}	$\Delta H_{L,NA}$	T_{IN}	δT_{IN}	McMillan ratio
$X = 0.00$	350.83	0.038	1.47	0.18	353.03	0.09	0.994
$X = 0.01$	349.79	0.030	1.18	0.12	353.63	0.13	0.989
$X = 0.02$	347.85		0.86		353.72	0.17	0.983
$X = 0.03$	346.22		0.68		354.33	0.14	0.977
$Y = 0.00$	340.18		0.40		353.38	0.06	0.963
$Y = 0.01$	338.65		0.33		354.08	0.07	0.956
$Y = 0.02$	337.81		0.31		354.78	0.11	0.952
$Y = 0.03$	335.66		0.29		355.45	0.14	0.944
$Y = 0.05$	333.76		0.27		355.96	0.56[a]	0.938

[a] This value is less reliable because only data with relatively fast scan-rates ($\sim$ 4 K/h) are available near the I-N transition for this mixture.

However, this is rather artificial because A^-/A^+ values are dependent on the data range. The quality of the fit has been improved in the sense of χ^2 values after inclusion of the corrections-to-scaling terms, while α remains insensitive to the data range. As displayed in Fig. 8, the fit with $|t|_{\max} = 0.003$ shows a good agreement with the experimental data. Thus we see that the $D_1^\pm$ and $D_2^\pm$ terms play an important role. $A^-/A^+ \sim 1$ has been obtained by taking the corrections-to-scaling terms into account. The first corrections-to-scaling terms show a good agreement with the theoretical expectation that $D_1^-/D_1^+ \sim 1$. As described above, α values are close to 0.5, indicating that there is no Fisher renormalization of the critical exponent. This also implies that the first corrections-to-scaling terms $A^\pm D_1^\pm |t|^{\theta-\alpha}$ reduce to be almost temperature independent. Hence, we rewrite Eq. (5) as the following expression:

$$\Delta C_p = A^\pm |t|^{-\alpha} \left(1 + D_2^\pm |t|\right) + B^\pm. \tag{6}$$

The obtained adjustable parameters are summarized in Table III. Values of α and T_c are more or less the same as those obtained using Eq. (5). The fits with $D_2^\pm = 0$ show poor χ^2 values, especially for large $|t|_{\max}$ fits, while the quality of the fit has been improved by taking the $D_2^\pm$ term into account.

The results of the fits for the $X = 0.03$ mixture are shown in Table IV. The critical exponent lies in $\alpha = 0.23 - 0.30$. These α values are nonuniversal, being between α_{XY} and $\alpha_{\rm TCP}$, and clearly small compared to those of the $X = 0.01$ mixture. The amplitude ratio A^-/A^+ still lies $\sim$1. For the $X = 0.03$ mixture, the fits with the corrections-to-scaling terms sometimes exhibit unphysical results for which the $D_1^\pm$ and $D_2^\pm$ values are very large. In those cases the T_c values slightly differ from the fits in which the leading exponent term is dominant or the $D_1^\pm$ are fixed to zero. To avoid such artifacts, fits were made with T_c value fixed at 346.226 K. As the result, the $D_1^\pm$ and $D_2^\pm$ terms become small and relatively stable. When $D_1^\pm$ terms are included, D_1^-/D_1^+ values are close to 1, and the quality of the fit is improved. Moreover, it is to be noted that the magnitude of the $D_1^\pm$ terms becames smaller than that of the $X = 0.01$ mixture. For other BC12/9OCB mixtures, the values of α decreased monotonically with the increase in X, although the detailed results are not shown. With decreasing X, it was also found that the corrections-to-scaling terms equally play an important role while their magnitude becomes smaller.

Table V shows the results for the $Y = 0.01$ mixture. For the fits with $D_2^\pm = 0$, the obtained α values range in 0.064–0.21, which is smaller than that for 8OCB. It is seen that the magnitude of $D_1^\pm$ decreases further compared to the $X = 0.03$ sample. On the other hand, A^+/A^- is still close to 1, implying the symmetric character of the heat capacity anomaly. The last two lines in the table show results with nonzero $D_2^\pm$. Quality

TABLE II. Results of the fits to the heat capacity data for the $X = 0.01$ mixture using Eq. (5). The minimum reduced temperatures used in the fits for $T > T_c$ and $T < T_c$ are $|t|^+_{\min} = 6.6 \times 10^{-5}$ and $|t|^-_{\min} = 4.6 \times 10^{-5}$, respectively. The units for A^+ and B_c are JK^{-1} g^{-1}.

$\|t\|_{\max}$	α	T_c	A^+	A^-/A^+	D_1^+	D_1^-/D_1^+	D_2^+	D_2^-/D_2^+	B_c	χ^2
0.0005	0.574	349.804	0.0112	0.955					−0.124	3.36
0.0010	0.545	349.804	0.0152	0.951					−0.207	5.13
0.0030	0.536	349.803	0.0170	0.923					−0.232	13.47
0.0050	0.535	349.803	0.0172	0.921					−0.234	12.56
0.0030	0.542	349.806	0.0144	1.074	19.45	0.67			−0.524	1.02
0.0050	0.559	349.806	0.0119	1.071	30.19	0.77			−0.642	2.33
0.0070	0.561	349.805	0.0121	1.018	23.13	0.84			−0.549	6.31
0.0050	0.474	349.807	0.0324	1.118	149.40	0.84	−99.14	0.24	−4.349	1.46
0.0070	0.453	349.807	0.0416	1.117	98.37	0.82	−103.99	0.16	−3.352	1.79

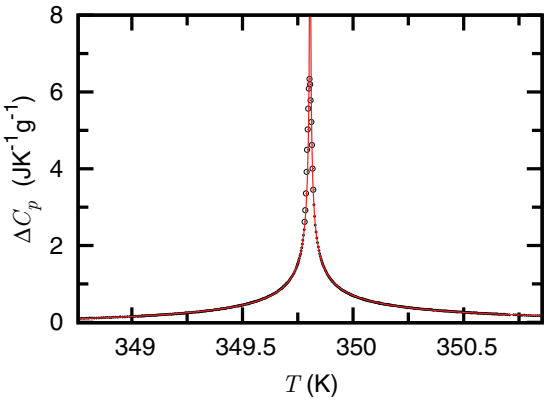

FIG. 8. (Color online) Temperature variation of the anomalous heat capacity near the N-SmA_d phase transition for $X = 0.01$. The solid line shows a fit to ΔC_p with Eq. (5). Open circles show the data omitted from the least-squares-fitting procedure.

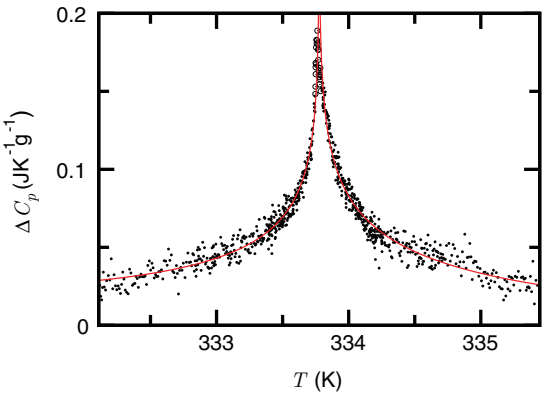

FIG. 9. (Color online) Temperature variation of the anomalous heat capacity near the N-SmA_d phase transition for $Y = 0.05$. The solid line shows a fit to ΔC_p with Eq. (5) with α and T_c fixed at -0.0066 and 333.777 K. Open circles show the data omitted from the least-squares-fitting procedure.

of the fits has been improved in the χ^2 sense. The α values are close to 0 and seem reasonable because they agree with those for $D_2^{\pm} = 0$ over narrower data ranges such as $|t|_{\max} = 0.003$.

The results for the $Y = 0.05$ mixture are summarized in Table VI. For the simple power-law fits with the corrections to scaling terms fixed to zero, the α values range between -0.019 and 0.138. It should be noted that the magnitude of the excess heat capacity is small compared to other data, as displayed in Fig. 5, and therefore the obscurity for determination of the critical exponent is inevitable. Because of this, fits with T_c fixed at 333.777 K have been tried. Fits were also made with the 3D-XY critical exponent $\alpha = \alpha_{XY} = -0.0066$. Figure 9 shows the result obtained with T_c = 333.777 K and $\alpha = \alpha_{XY}$. The quality of the fits with both α and T_c fixed are comparable with the fits with parameters adjusted freely. On the other hand, no clear evidence of the 3D-XY critical amplitude ratio has been found, and the A^-/A^+ values still remain close to 1.

III. DISCUSSION

Our calorimetric studies revealed that the N-SmA_d phase transition is first order for pure 9OCB, which agree with the result obtained by means of a modulated DSC technique [25]. For the $X = 0.01$ mixture, it has been found that the transition is very weakly first order. Other mixtures exhibit second-order transitions. The behavior of the phase signal ϕ in the ac technique has been used for the distinction between first- and second-order transitions. However, it should be stressed that the ac calorimetric technique cannot determine the transitional enthalpy, and the response of ϕ is rather insensitive to the small latent heat. The C_p data obtained by ac calorimetry sometimes show a remarkable difference from those of DSC [26]. Thus, the direct measurement of the transition enthalpy would be reliable information. So far, the adiabatic calorimetry is suitable for this requirement [27,28]. Compared with this, as far as the the earlier DSC measurements are concerned, because of the dynamic temperature scan incapable of detecting the heat flow difference instantaneously, it was difficult to clearly distinguish between first- and second-order transitions. In the present study, our high-sensitivity DSC allowed us to give a fairly good agreement of DSC and ac calorimetry data, providing a reliable evidence to distinguish between first- and second-order transitions.

Nearly tricritical behavior has been observed for the $X = 0.01$ mixture. The value of McMillan ratio $r = 0.99$ for this mixture is in a good agreement with that of the previously reported value at the tricritical point of the N-SmA_d phase transition. The obtained α values, slightly larger than $\alpha_{\rm TCP} = 0.5$, may be due to the weakly first-order character. From the viewpoint of α values, the observation of the Fisher renormalization in the present work should be the most pronounced for $X = 0.01$ due to the doubling of the critical exponent at the tricritical point. The value of

TABLE III. Results of fits to the heat capacity data for the $X = 0.01$ mixture using Eq. (6). The minimum reduced temperatures used in the fits for $T > T_c$ and $T < T_c$ are $|t|^+_{\min} = 6.6 \times 10^{-5}$ and $|t|^-_{\min} = 4.6 \times 10^{-5}$, respectively. The units for A^+ and $B^{\pm}$ are JK^{-1} g^{-1}.

$\lvert t\rvert_{\max}$	α	T_c	A^+	A^-/A^+	D_2^+	D_2^-/D_2^+	B^+	B^-/B^+	χ^2
0.0005	0.554	349.805	0.0134	1.002			−0.155	1.24	2.14
0.0030	0.529	349.806	0.0169	1.062			−0.193	1.52	1.02
0.0050	0.528	349.806	0.0171	1.052			−0.200	1.44	2.56
0.0070	0.533	349.805	0.0167	1.006			−0.208	1.27	6.60
0.0030	0.537	349.806	0.0155	1.063	−19.50	0.98	−0.159	1.62	1.00
0.0050	0.523	349.807	0.0173	1.142	−38.51	−1.23	−0.155	2.37	1.49
0.0070	0.522	349.807	0.0174	1.158	−49.91	−1.30	−0.146	2.69	1.94

TABLE IV. Results of fits to the heat capacity data for the $X = 0.03$ mixture using Eq. (5). The minimum reduced temperatures used in the fits for $T > T_c$ and $T < T_c$ are $|t|^+_{\rm min} = 9.5 \times 10^{-5}$ and $|t|^-_{\rm min} = 1.4 \times 10^{-4}$, respectively. The units for A^+ and B_c are $\mathrm{JK^{-1}\,g^{-1}}$. Quantities in brackets are held fixed at the given values.

$\lvert t\rvert_{\rm max}$	α	T_c	A^+	A^-/A^+	D_1^+	D_1^-/D_1^+	D_2^+	D_2^-/D_2^+	B_c	χ^2
0.0010	0.292	[346.226]	0.0675	1.017					−0.229	1.76
0.0010	0.260	346.224	0.0977	1.006					−0.310	1.29
0.0050	0.269	[346.226]	0.0891	1.006					−0.293	5.00
0.0050	0.252	346.222	0.1076	0.993					−0.331	2.96
0.0030	0.302	346.226	0.0552	1.044	−5.539	1.17			−0.087	1.43
0.0050	0.241	[346.226]	0.1252	1.034	1.885	0.48			−0.422	1.44
0.0070	0.231	346.226	0.1439	1.032	2.391	0.61			−0.484	1.38

$Z \equiv (T_c^{-1} \cdot dT_c/dx)^2$ in Eq. (1) is a suitable measure to characterize the observability of the renormalized exponent. Previously, fully Fisher-renormalized tricritical behaviors show Z values ranging from 0.74 to 0.2 [9,10,29]. In the present study, $Z \sim 0.18$ for $X = 0.01$ seems sufficient for the appearance of the crossover temperature. However, according to the analysis described above, no sign of the Fisher renormalization has been obtained. By substituting the parameters to Eq. (1) using the critical amplitude $A^{\pm}$ in Table II, the range of the crossover in the reduced temperature becomes $\tau \sim 10^{-6}$. This indicates that the observable region is quite narrow, in accordance with our analysis. The present result can be compared with our recent study in a different system, which revealed that a Fisher-renormalized behavior actually occurs in the vicinity of T_c [13]. In that case the system also included a tricritical point and a steep phase boundary, which is apparently similar to those in the present study. The crucial difference lies in the dilute composition of the bent-shaped molecules used here. Hence, we see that the concentration is also a very important factor to determine the crossover temperature.

The present results confirm that the width of the nematic temperature range plays an important role for deciding the nature of the N-SmA phase transition. First, the magnitude of the heat capacity anomaly decreases significantly as the nematic range grows, showing that thermal fluctuations associated with the heat capacity anomaly are very sensitive to the saturation of the nematic order, as pointed out in our previous work [13] and also in earlier works cited therein (see Ref. [30], for instance).

The trend of the critical behavior as a function of the nematic range also deserves attention. The critical behavior for $X = 0.02$ and 0.03 mixtures, pure 8OCB, and $Y = 0.01$–0.03 mixtures exhibit nonuniversal exponents between the 3D-XY and tricritical values. For $X = 0.05$, the excess heat capacity anomaly is well described with the 3D-XY critical exponent. The amplitude ratio showing the symmetric feature is more analogous to that of the nCB series [27,28] than that of the nonpolar mixtures exhibiting nonuniversal tricritical amplitude [29]. The relation between α and T_{NA}/T_{IN} is shown in Fig. 10. The overall behavior approaching the 3D-XY value is in remarkable agreement with the previous reports on the N-SmA phase transitions [31], which are shown in the figure as inverted triangles and open circles. We also mention here that this crossover of α gives rise to characteristic behavior regarding the magnitude of the first-order corrections-to-scaling terms $D_1^{\pm}$. Their values clearly diminish as the decrease of α values

TABLE V. Results of fits to the heat capacity data for the $Y = 0.01$ mixture using Eq. (5). The minimum reduced temperatures used in the fits for $T > T_c$ and $T < T_c$ are $|t|^+_{\rm min} = 7.4 \times 10^{-5}$ and $|t|^-_{\rm min} = 5.9 \times 10^{-6}$, respectively. The units for A^+ and B_c are $\mathrm{JK^{-1}\,g^{-1}}$. Quantities in brackets are held fixed at the given values.

$\lvert t\rvert_{\rm max}$	α	T_c	A^+	A^-/A^+	D_1^+	D_1^-/D_1^+	D_2^+	D_2^-/D_2^+	B_c	χ^2
0.0005	0.153	338.663	0.1237	1.027					−0.267	1.22
0.0010	0.135	338.664	0.1576	1.038					−0.312	1.36
0.0030	0.151	338.665	0.1159	1.062					−0.239	1.56
0.0050	0.158	338.665	0.1041	1.069					−0.220	1.52
0.0070	0.162	338.665	0.0980	1.071					−0.210	1.47
0.0030	0.124	[338.663]	0.2147	1.003	1.654	1.76			−0.444	1.05
0.0030	0.064	[338.664]	0.7147	1.006	1.201	1.37			−1.067	1.06
0.0050	0.167	[338.663]	0.1035	1.011	0.807	3.06			−0.248	1.07
0.0050	0.109	[338.664]	0.2668	1.014	1.354	1.54			−0.502	1.09
0.0070	0.211	[338.663]	0.0526	1.023	−1.589	−0.30			−0.125	1.17
0.0070	0.147	[338.664]	0.1351	1.027	0.848	2.00			−0.294	1.18
0.0070	0.032	[338.663]	2.1828	0.997	1.075	1.50	−3.239	2.69	−2.720	0.95
0.0070	−0.021	[338.664]	−5.3621	1.000	−0.753	1.35	2.629	2.06	4.626	0.97

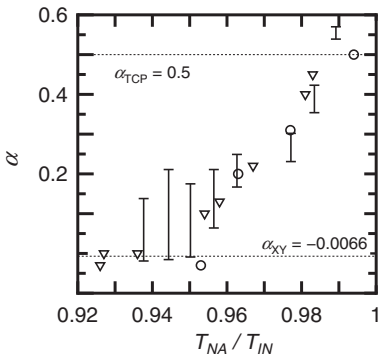

FIG. 10. Specific heat critical exponent α plotted against the McMillan ratio. The α values displayed here have been obtained from fits without $D_2^{\pm}$ terms. Results reported in Ref. [31] for N-SmA_m transitions (inverted triangles) and for N-SmA_d transitions (open circles) are also shown.

as shown in Table II–VI. It is seen that $D_1^{\pm}$ values for the $X = 0.01$ mixture are much larger than those for the $Y = 0.05$ mixture. Although it is known that $D_1^{\pm}$ values are nonuniversal, we can speculate that this trend reflects the change in α. If α is closer to 0.5, the distinction between $D_1^{\pm}|t|^{\theta-\alpha}$ and B_c becomes difficult because they are almost constant terms. Contrary to the tricritical case, the heat capacity anomaly for $X = 0.05$ with smaller α can exhibit the clear temperature dependence of $D_1^{\pm}|t|^{\theta-\alpha}$. Moreover, the magnitude of $D_1^{\pm}$ terms for $Y = 0.05$ is in reasonable agreement with other liquid crystal samples exhibiting the 3D-XY critical behavior [32].

In contrast to the crossover of the critical exponent, the critical amplitude ratio shows no clear evidence that A^-/A^+ agrees with the 3D-XY value of 0.971 or the inverted value of 1.027. Experimentally, the well-described XY-like behaviors were observed for the cases with a large nematic range of $T_{NA}/T_{IN} < 0.90$ [31]. There, heat capacity anomalies above and below T_c show clearly asymmetric character. Contrary to those previous reports, the present data are symmetric and inconsistent with both $A^-/A^+ < 1$ and $A^-/A^+ > 1$. A plausible reason may be attributable to an interaction between director fluctuations δn and the smectic order parameter [33]. This anisotropic effect gives rise to deviations from isotropic XY behavior when the nematic range is small. In this sense the $T_{NA}/T_{IN} = 0.937$ is still not sufficient to produce the asymmetric heat capacity anomaly.

The fact that the nematic range is widened significantly by inclusion of bent-shaped molecules is quite remarkable, and a deeper discussion is warranted. In the present work, since the mole fractions of the doped bent-shaped molecules are quite small, they can be regarded as impurities. Apparently similar widening of nematic phase was reported by Denolf *et al.* [34]. They explained the linear temperature dependence for the N-SmA and I-N phase transitions by taking the coupling between the orientational order parameter S and the mole fraction of the impurities. However, they always observed a downward shift of transition temperatures in contrast to the present result, where the I-N transition increases significantly with X and Y. Such a difference seems natural because nonmesogenic impurities have been used in their work, while in our case the dopant molecules have the capability of forming liquid crystal phases by themselves. It is of particular interest that the inclusion of BC12 stabilizes the nematic phase and destabilizes the Sm-A_d phase. It is possible that the more rigid core of the BC12 dopant dampens director fluctuations. The question arises if the bent-core nature of BC12 plays a role, or if a linear rigid core molecule of similar character produces equal effects. A linear-core version of BC12 may not stabilize the Sm-A phase to the same extent but may perhaps stabilize the nematic phase more, leading to a more or less alike nematic range. Such possibilities will be interesting candidates for future studies.

TABLE VI. Results of fits to the heat capacity data for the $Y = 0.05$ mixture using Eq. (5). The minimum reduced temperatures used in the fits for $T > T_c$ and $T < T_c$ are $|t|^+_{\min} = 2.6 \times 10^{-6}$ and $|t|^-_{\min} = 6.3 \times 10^{-5}$, respectively. The units for A^+ and B_c are $\mathrm{JK^{-1}\,g^{-1}}$. Quantities in brackets are held fixed at the given values.

$\lvert t\rvert_{\max}$	α	T_c	A^+	A^-/A^+	D_1^+	D_1^-/D_1^+	D_2^+	D_2^-/D_2^+	B_c	χ^2
0.0010	[−0.0066]	333.777	−5.196	1.002					5.036	1.03
0.0010	−0.019	333.777	−1.991	1.006					1.817	1.03
0.0030	[−0.0066]	333.783	−4.762	1.001					4.620	1.33
0.0030	0.138	333.777	0.080	0.974					−0.137	1.22
0.0050	0.129	333.778	0.091	0.979					−0.152	1.24
0.0070	0.115	333.779	0.113	0.985					−0.180	1.26
0.0010	[−0.0066]	333.775	−5.074	1.004	0.052	−0.42			4.926	1.00
0.0030	[−0.0066]	[333.777]	−6.369	1.003	−0.094	1.53			6.137	1.10
0.0030	[−0.0066]	333.775	−6.443	1.003	−0.093	1.63			6.208	1.09
0.0050	[−0.0066]	[333.777]	−6.005	1.002	−0.075	1.51			5.794	1.16
0.0050	0.004	[333.777]	9.037	0.999	0.043	1.55			−9.233	1.16
0.0050	[−0.0066]	333.775	−6.039	1.003	−0.073	1.60			5.827	1.16
0.0070	[−0.0066]	[333.777]	−5.767	1.002	−0.061	1.54			5.570	1.20
0.0070	0.073	[333.777]	0.262	0.974	0.209	3.01			−0.366	1.19
0.0070	[−0.0066]	333.776	−5.785	1.002	−0.061	1.58			5.587	1.20
0.0070	[−0.0066]	[333.777]	−6.522	1.003	−0.120	1.81	0.289	3.58	6.279	1.16
0.0070	[−0.0066]	333.775	−6.675	1.004	−0.121	1.97	0.273	4.42	6.424	1.14

In summary, we have measured the heat capacity near the N-SmA_d phase transition in mixtures with a small amount of the bent-shaped molecules. The critical exponent analyses revealed that the tricritical exponent crosses over toward the XY-like value with the increase of the nematic temperature range. On the other hand, despite the sharp change of the transition temperatures with the mixing ratio, no feature of the Fisher renormalization of the critical exponent has been seen. This result confirms the expectation that the smallness of the concentration plays a significant role in the observability of the renormalized region.

ACKNOWLEDGMENTS

The authors are grateful to D. Miyajima and T. Aida for kindly supplying the liquid crystal samples. This research was supported by the G-COE programs (Nanoscience and Quantum Physics, Education and Research Center for Material Innovation) at the Tokyo Institute of Technology.

[1] R. Pratibha, N. Madhusudana, and B. Sadashiva, Science **288**, 2184 (2000).
[2] R. Pratibha, N. V. Madhusudana, and B. K. Sadashiva, Phys. Rev. E **71**, 011701 (2005).
[3] T. Otani, F. Araoka, K. Ishikawa, and H. Takezoe, J. Am. Chem. Soc. **131**, 12368 (2009).
[4] C. Zhu, D. Chen, Y. Shen, C. D. Jones, M. A. Glaser, J. E. Maclennan, and N. A. Clark, Phys. Rev. E **81**, 011704 (2010).
[5] Y. Takanishi, Y. Ohtsuka, Y. Takahashi, and A. Iida, Phys. Rev. E **81**, 011701 (2010).
[6] M. E. Fisher, Phys. Rev. **176**, 257 (1968).
[7] M. E. Fisher and P. E. Scesney, Phys. Rev. A **2**, 825 (1970).
[8] J. P. Hill, B. Keimer, K. W. Evans-Lutterodt, R. J. Birgeneau, and C. W. Garland, Phys. Rev. A **40**, 4625 (1989).
[9] M. E. Huster, K. J. Stine, and C. W. Garland, Phys. Rev. A **36**, 2364 (1987).
[10] J. Caerels, C. Glorieux, and J. Thoen, Phys. Rev. E **65**, 031704 (2002).
[11] D. A. Huse, Phys. Rev. Lett. **55**, 2228 (1985).
[12] P. Das, G. Nounesis, C. Garland, G. Sigaud, and N. Tinh, Liq. Cryst. **7**, 883 (1990).
[13] Y. Sasaki, K. Ema, K. V. Le, H. Takezoe, S. Dhara, and B. K. Sadashiva, Phys. Rev. E **82**, 011709 (2010).
[14] E. Bloemen, J. Thoen, and W. Van Dael, J. Chem. Phys. **75**, 1488 (1981).
[15] M. A. Anisimov, A. V. Voronel, and E. E. Gorodetskiĭ, Sov. Phys. JETP **33**, 605 (1971).
[16] C. Bagnuls and C. Bervillier, Phys. Rev. B **32**, 7209 (1985).
[17] C. Bervillier, Phys. Rev. B **34**, 8141 (1986).
[18] K. Ema and H. Yao, Thermochim. Acta **304/305**, 157 (1997).
[19] C. W. Garland, Thermochim. Acta **88**, 127 (1985).
[20] K. Ema, G. Nounesis, C. W. Garland, and R. Shashidhar, Phys. Rev. A **39**, 2599 (1989).
[21] H. Haga and C. W. Garland, Liq. Cryst. **23**, 645 (1997).
[22] K. Ema, M. Kanai, H. Yao, Y. Takanishi, and H. Takezoe, Phys. Rev. E **61**, 1585 (2000).
[23] C. Bagnuls, C. Bervillier, D. I. Meiron, and B. G. Nickel, Phys. Rev. B **35**, 3585 (1987).
[24] J. A. Potton and P. C. Lanchester, Phase Transit. **6**, 43 (1985).
[25] P. Cusmin, M. de la Fuente, J. Salud, M. Perez-Jubindo, S. Diez-Berart, and D. Lopez, J. Phys. Chem. B **111**, 8974 (2007).
[26] Y. Sasaki, Y. Setoguchi, H. Nagayama, H. Yao, H. Takezoe, and K. Ema, Physica E **43**, 779 (2011).
[27] J. Thoen, H. Marynissen, and W. Van Dael, Phys. Rev. Lett. **52**, 204 (1984).
[28] H. Marynissen, J. Thoen, and W. Van Dael, Mol. Cryst. Liq. Cryst. **124**, 195 (1985).
[29] K. J. Stine and C. W. Garland, Phys. Rev. A **39**, 3148 (1989).
[30] D. Brisbin, R. DeHoff, T. E. Lockhart, and D. L. Johnson, Phys. Rev. Lett. **43**, 1171 (1979).
[31] C. W. Garland and G. Nounesis, Phys. Rev. E **49**, 2964 (1994).
[32] C. W. Garland, G. Nounesis, and K. J. Stine, Phys. Rev. A **39**, 4919 (1989).
[33] B. R. Patton and B. S. Andereck, Phys. Rev. Lett. **69**, 1556 (1992).
[34] K. Denolf, G. Cordoyiannis, C. Glorieux, and J. Thoen, Phys. Rev. E **76**, 051702 (2007).